FINITE ELEMENT METHOD FOR COUPLED DYNAMIC FLOW-DEFORMATION SIMULATION

J.M. van Esch
Department of Geo-engineering, Deltares, Delft, The Netherlands

D. Stolle
Department of Civil Engineering, McMaster University, Hamilton, ON, Canada

I. Jassim
Institute of Geotechnical Engineering, Stuttgart University, Stuttgart, Germany

ABSTRACT: *This article compares a solid velocity - liquid velocity formulation and a solid velocity - liquid pressure formulation for solving the coupled flow and deformation problem in an elastic media. The finite element formulations presented here apply to small deformations, but are in the process of being extended to large deformations within a material point formulation. As the material point model uses low-order elements and forward integration in time, the finite element model has to be composed accordingly. Dynamic simulations presented in this paper focus on capturing the first compression wave, which loads the liquid phase and solid phase, and on resolving the second compression wave, which starts the consolidation process. Whereas the velocity - velocity formulation properly captures two-phase dynamic behavior including the second wave, the velocity - pressure formulation is not capable of capturing the second compression wave. With regards to implementation within a material point framework, the first formulation is more consistent in the treatment of the solid and liquid phases, providing a physically based mapping of momentum for both phases, and is preferred for this reason.*

1 INTRODUCTION

Considerable research has been carried out to address problems that involve soil-pore fluid interaction that include, for example, those dealing with consolidation, liquefaction and wave loading. The equations describing two-phase flow were originally developed by Biot (1956a), Biot (1956b), with Zienkiewicz & Shiomi (1984) and Zienkiewicz et al. (1990) investigating the numerical implementation in terms of various formulations. For a comprehensive review of the various formulations within the context of mixture theory, the reader is referred to Gidaspow (1994). A more recent contribution relevant to this paper is presented by Jeremic et al. (2008). Various simplifications have been introduced depending on the rate of loading, the dissipation time of excess pore pressure, and the speed of shear and compression waves within the media. One must however realize that each term that is eliminated introduces an error, which is spread over the other terms. As a result, certain non-physical behaviors may be captured, which in turn could lead to a misinterpretation of results and erroneous conclusions. This paper briefly reviews the two-phase flow equations and then presents a series of one-dimensional examples to demonstrate the significance of various simplifications. The emphasis is placed on use of explicit time-stepping schemes that are well-suited for implementation in material point method models.

2 MATHEMATICAL MODEL

The mathematical model provides the governing equations for coupled flow and deformation within a domain of interest Ω that is closed by its boundary Γ. Equations are given for Cartesian coordinates $x_i\,(\mathrm{m})$, with time denoted by $t\,(\mathrm{s})$. Throughout this section the index notation is used. Subscripts denote vector or tensor components in the coordinate system. Superscripts 's' and 'l' represent solid and liquid components of the variables respectively for the two-phase dynamical problem.

2.1 Balance Equations

This section presents the mass balance equations and the momentum balance equations for the liquid phase and the solid phase separately as outlined by Verruijt (2010). The equilibrium equation and the storage equation follow as a combination of the balance equations completed by constitutive laws. The mass balance equation for the solid phase reads

$$\frac{\partial}{\partial t}\left[(1-n)\,\rho^s\right] + \frac{\partial}{\partial x_i}\left[(1-n)\,\rho^s v_i\right] = 0, \tag{1}$$

where $\rho^s\,(\mathrm{kg/m^3})$ is the density of the solid phase material, $n\,(-)$ denotes porosity, which is dimensionless, and $v_i\,(\mathrm{m/s})$ represents the velocity vector of the solid phase material corresponding to the x_i direction. The momentum balance for the solid phase reads

$$(1-n)\rho^s\frac{\partial v_j}{\partial t} - \frac{\partial \sigma'_{ij}}{\partial x_i} - (1-n)\frac{\partial p}{\partial x_j} - (1-n)\rho^s g_j - n^2\mu\kappa^{-1}_{ji}\,(w_i - v_i) = 0. \tag{2}$$

Here $\sigma'_{ij}\,(\mathrm{N/m^2})$ denotes the effective stress tensor in the solid skeleton (positive for tension), $p\,(\mathrm{N/m^2})$ is the pressure in the liquid phase (positive for suction), and $g_j\,(\mathrm{m/s^2})$ indicates the gravitational acceleration vector. The dynamic viscosity of the liquid is given by $\mu\,(\mathrm{kg\,m/s^2})$, the components of the inverse of the intrinsic permeability tensor are denoted by $\kappa^{-1}_{ij}\,(\mathrm{m^2})$, and the velocity of the liquid phase is written as $w_i\,(\mathrm{m/s})$. Conservation of moment of momentum requires $\sigma'_{ij} = \sigma'_{ji}$. The mass balance for the liquid is given by

$$\frac{\partial}{\partial t}\left(n\rho^l\right) + \frac{\partial}{\partial x_i}\left(n\rho^l w_i\right) = 0, \tag{3}$$

with $\rho^l\,(\mathrm{kg/m^3})$ being the density of the pore water. The momentum balance for the liquid reads

$$n\rho^l\frac{\partial w_j}{\partial t} - n\frac{\partial p}{\partial x_j} - n\rho^l g_j + n^2\mu\kappa^{-1}_{ji}\,(w_i - v_i) = 0. \tag{4}$$

Since displacements are small and we are following the material in the material point method, time derivatives replace material derivatives in this formulation.

2.2 Equilibrium Equation

The momentum balance for the mixture follows from adding Eqs. (2) and (4) yielding

$$(1-n)\,\rho^s\frac{\partial v_j}{\partial t} + n\rho^l\frac{\partial w_j}{\partial t} - \frac{\partial \sigma_{ij}}{\partial x_i} - \gamma_j = 0, \tag{5}$$

where $\sigma_{ij}\,(\mathrm{N/m^2})$ represents the total stress tensor, and $\gamma_j\,(\mathrm{N/m^3})$ is the unit weight of the mixture. The density of the soil mixture $\rho\,(\mathrm{kg/m^3})$ reads $\rho = (1-n)\,\rho^s + n\rho^l$; thus $\gamma_j = \rho g_j$. The effective stress is related to the total stress and pore pressure by the Terzaghi decomposition according to

$$\sigma_{ij} = \sigma'_{ij} + \delta_{ij} p, \tag{6}$$

where $\delta_{ij}\,(-)$ is the Kronecker delta operator. For an elastic material the constitutive equation is defined as

$$\sigma'_{ij} = D_{ijkl}\epsilon_{kl}, \tag{7}$$

where $D_{ijkl}\,(\mathrm{N/m^2})$ represents the fourth order material stiffness tensor, and $\epsilon_{kl}\,(-)$ expresses the second order strain tensor. For an isotropic elastic material the stiffness tensor components are given by

$$D_{ijkl} = \mu^e\left(\delta_{ik}\delta_{jl} + \delta_{il}\delta_{jk}\right) + \lambda^e \delta_{ij}\delta_{kl}, \tag{8}$$

where $\mu^e\,(\mathrm{N/m^2})$ and $\lambda^e\,(\mathrm{N/m^2})$ are the Lamé constants. Assuming small deformations, the strain-displacement relation gives

$$\epsilon_{ij} = \tfrac{1}{2}\left(\frac{\partial u_i}{\partial x_j} + \frac{\partial u_j}{\partial x_i}\right). \tag{9}$$

The velocity of the solid phase relates to the displacement of the solid phase $u_i\,(\mathrm{m})$ as $v_i = \partial u_i/\partial t$.

2.3 Storage Equation

Assuming spatial variations in the liquid density and the porosity are negligible, the mass balance equation (3) for the liquid phase yields

$$n\frac{\partial \rho^l}{\partial t} + \rho^l \frac{\partial n}{\partial t} + n\rho^l \frac{\partial w_i}{\partial x_i} = 0. \tag{10}$$

Solid particles are assumed to by incompressible. Neglecting the gradient of the porosity in the mass balance equation (1) for the solid phase gives

$$\frac{\partial n}{\partial t} - (1-n)\frac{\partial v_i}{\partial x_i} = 0. \tag{11}$$

Inserting Eq. (11) into the mass balance equation (10) for the liquid phase then gives

$$\frac{n}{\rho^l}\frac{\partial \rho^l}{\partial t} + (1-n)\frac{\partial v_i}{\partial x_i} + n\frac{\partial w_i}{\partial x_i} = 0, \tag{12}$$

which is the volumetric form of the combined mass balance equation. The proposed constitutive relation for the density of the liquid reads

$$\frac{d\rho^l}{dp} = -\beta\rho^l, \tag{13}$$

where $\beta\,(\mathrm{m^2/N})$ is the compressibility of the liquid (pressure is negative for compression), which corresponds to the inverse of the compression modulus of the liquid phase. Defining specific discharge $q_i\,(\mathrm{m/s})$ as

$$q_i = n\left(w_i - v_i\right), \tag{14}$$

the mass balance equation (12) can be written as

$$n\beta\frac{\partial p}{\partial t} - \frac{\partial q_i}{\partial x_i} - \frac{\partial v_i}{\partial x_i} = 0, \tag{15}$$

with the momentum balance equation (4) reformulated as

$$q_i = \frac{\kappa_{ij}}{\mu}\left(\frac{\partial p}{\partial x_j} + \rho^l g_j - \rho^l \frac{\partial w_j}{\partial t}\right). \tag{16}$$

The storage equation then follows from Eqs. (15) and (16) as

$$n\beta\frac{\partial p}{\partial t} - \frac{\partial}{\partial x_i}\left[\frac{\kappa_{ij}}{\mu}\left(\frac{\partial p}{\partial x_j} + \rho^l g_j - \rho^l \frac{\partial w_j}{\partial t}\right)\right] - \frac{\partial v_i}{\partial x_i} = 0. \tag{17}$$

3 Solid Velocity - Liquid Pressure ($v - p$) Formulation

The $v - p$ formulation considers the relative velocity ($q \neq 0$). However the acceleration of the solid phase is assumed to equal to the acceleration of the liquid phase ($\partial v/\partial t \approx \partial w/\partial t$). The momentum balance equation (5) for the mixture then reads

$$\rho\frac{\partial v_j}{\partial t} = \frac{\partial \sigma_{ij}}{\partial x_i} + \gamma_j \qquad \text{in} \quad \Omega, \tag{18}$$

and the storage equation (17) can be written as

$$n\beta\frac{\partial p}{\partial t} = \frac{\partial}{\partial x_i}\left[\frac{\kappa_{ij}}{\mu}\left(\frac{\partial p}{\partial x_j} + \rho^l g_j - \rho^l \frac{\partial v_j}{\partial t}\right)\right] + \frac{\partial v_i}{\partial x_i} \qquad \text{in} \quad \Omega. \tag{19}$$

The effective stress increment follows from Eq. (7) and Eq. (8) as

$$\frac{\partial \sigma'_{ij}}{\partial t} = \tfrac{1}{2} D_{ijkl}\left(\frac{\partial v_k}{\partial x_l} + \frac{\partial v_l}{\partial x_k}\right) \qquad \text{in} \quad \Omega. \tag{20}$$

For this set of equations the primary variables are: velocity of the solid phase v_i, pressure in the liquid phase p, and effective stress in the solid phase σ'_{ij}. Dirichlet boundary conditions prescribe a velocity $\overline{v}_i$ for the solid phase according to

$$v_i = \overline{v}_i \qquad \text{on} \quad \Gamma_1^v, \tag{21}$$

and a pressure $\overline{p}$ for the liquid phase by

$$p = \overline{p} \qquad \text{on} \quad \Gamma_1^p \tag{22}$$

Cauchy boundary conditions for the solid phase prescribe a traction as

$$\sigma_{ij} n_j = \overline{\tau}_i \qquad \text{on} \quad \Gamma_2^v, \tag{23}$$

where $\overline{\tau}_i\,(\mathrm{N/m^2})$ denotes the traction vector components on the boundary, and $n_j\,(-)$ represents the outward pointing normal to the boundary. For the liquid phase Cauchy boundary conditions read

$$\frac{\kappa_{ij}}{\mu}\left(\frac{\partial p}{\partial x_j} + \rho^l g_j - \rho^l \frac{\partial w_j}{\partial t}\right) n_i = \overline{q}_i n_i \qquad \text{on} \quad \Gamma_2^p, \tag{24}$$

where $\overline{q}_i$ denotes the components of the outflux vector over the boundary.

The finite element method constructs the weak formulation of the given partial differential equations, and obtains the pressure in the liquid phase and the velocity of the solid phase at the nodes. In this article a Galerkin finite element discretization in space is adopted. The interpolation function $N_a\,(-)$ is used as the weighting function. An explicit finite difference time integration scheme is applied, and the mass matrices are lumped. The uncoupled set of equations are then solved sequentially. In this section discrete locations in space are indicated by the subscripts a and b. The superscript n denotes a point in time.

The discrete equilibrium equation follows from the momentum balance equation (18) of the mixture and provides the velocity increment Δv_j of the solid phase as

$$\int_\Omega \rho N_a \delta_{ab} \Delta v_{bj} d\Omega = -\Delta t \int_\Omega \frac{\partial N_a}{\partial x_i} \sigma_{ij}^n d\Omega + \Delta t \int_{\Gamma_2^u} N_a \overline{\tau}_{aj}^n d\Gamma + \Delta t \int_\Omega N_a \gamma_j d\Omega, \tag{25}$$

with the velocity of the solid phase at the next step in time following from the velocity at the current step and the velocity increment as $v_j^{n+1} = v_j^n + \Delta v_j$. The corresponding storage equation (19) discretizes to

$$\begin{aligned}\int_\Omega n\beta N_a \delta_{ab} \Delta p_b d\Omega = &-\Delta t \int_\Omega \frac{\kappa_{ij}}{\mu} \frac{\partial N_a}{\partial x_i} \frac{\partial N_b}{\partial x_j} p_b^n d\Omega - \Delta t \int_\Omega \frac{\kappa_{ij}}{\mu} \frac{\partial N_a}{\partial x_i} \rho g_j d\Omega \\ &+ \int_\Omega \frac{\kappa_{ij}}{\mu} \frac{\partial N_a}{\partial x_i} N_b \Delta v_{bi} d\Omega + \Delta t \int_{\Gamma_2^p} N_a \overline{q}_{ai}^n n_i d\Gamma + \int_\Omega N_a \frac{\partial N_b}{\partial x_i} \Delta u_{bi} d\Omega,\end{aligned} \tag{26}$$

and provides the pressure increment Δp, which increases the total stress $\Delta \sigma_{ij}$ according to

$$\Delta \sigma_{ij} = \tfrac{1}{2} \Delta t D_{ijkl} \left(\frac{\partial N_a}{\partial x_l} v_{ak}^{n+1} + \frac{\partial N_a}{\partial x_k} v_{al}^{n+1} \right) + \delta_{ij} N_a \Delta p_a. \tag{27}$$

Additionally, the Darcy velocity vector field at the next time step follows locally from

$$q_j^{n+1} = \frac{\kappa_{ji}}{\mu} \left(\frac{\partial N_a}{\partial x_j} p_a^{n+1} + \rho^l g_j - \rho^l N_a \frac{\Delta v_{aj}}{\Delta t} \right). \tag{28}$$

Stress updates $\sigma_{ij}^{n+1} = \sigma_{ij}^n + \Delta \sigma_{ij}$ and pressure updates $p^{n+1} = p^n + \Delta p$ are used to solve the set of algebraic equations sequentially.

4 Solid Velocity - Liquid Velocity ($v - w$) Formulation

The $u - w$ formulation follows the procedure outlined by Verruijt (2010), in which the increase of liquid phase velocity follows from Eq. (4) as

$$\rho^l \frac{\partial w_j}{\partial t} = \frac{\partial p}{\partial x_j} + \rho^l g_j - n\mu \kappa_{ij}^{-1} (w_i - v_i) \qquad \text{in} \quad \Omega. \tag{29}$$

Inserting this expression into Eq. (2) to obtain the solid phase velocity, yields

$$(1-n)\rho^s \frac{\partial v_j}{\partial t} = -n\rho^l \frac{\partial w_j}{\partial t} + \frac{\partial \sigma'_{ij}}{\partial x_i} + \frac{\partial p}{\partial x_j} + \rho g_j \qquad \text{in} \quad \Omega. \tag{30}$$

The pressure increase that follows from the mass balance equation (15), for the liquid phase and Eq. (14) for the relative velocity as

$$n\beta\frac{\partial p}{\partial t} = n\frac{\partial w_i}{\partial x_i} + (1-n)\frac{\partial v_i}{\partial x_i} \qquad \text{in} \quad \Omega, \tag{31}$$

with the effective stress increment follows from the velocity field of the solid phase according to

$$\frac{\partial \sigma'_{ij}}{\partial t} = \tfrac{1}{2}D_{ijkl}\left(\frac{\partial v_k}{\partial x_l} + \frac{\partial v_l}{\partial x_k}\right) \qquad \text{in} \quad \Omega. \tag{32}$$

For this set of equations the primary variables are: velocity of the solid phase v_i, velocity of the liquid phase w_i, pressure in the liquid phase p, and effective stress in the solid phase σ'_{ij}.

Dirichlet boundary conditions for the solid phase and liquid phase combine to

$$v_i = \overline{v}_i, \quad w_i = \overline{w}_i \qquad \text{on} \quad \Gamma_1. \tag{33}$$

Cauchy boundary conditions for the solid phase and for the liquid phase read

$$\sigma_{ij}n_j = \overline{\tau}_i, \quad pn_i = \overline{p}n_i \qquad \text{on} \quad \Gamma_2. \tag{34}$$

The finite element method obtains the velocity of the liquid phase and the velocity of the solid phase at the nodes. The weak form of Eq. (29) gives an expression for the velocity increment Δw_j of the liquid phase according to

$$\begin{aligned}\int_\Omega \rho^l N_a \delta_{ab}\Delta w_{bj} d\Omega = &-\Delta t\int_\Omega \frac{\partial N_a}{\partial x_j}p_a^n d\Omega + \Delta t\int_\Gamma N_a p_a^n n_j d\Gamma + \Delta t\int_\Omega \rho^l g_j N_a d\Omega \\ &- \Delta t\int_\Omega n\mu\kappa_{ij}^{-1}N_a\delta_{ab}\Delta w_{bj}^n d\Omega + \Delta t\int_\Omega n\mu\kappa_{ij}^{-1}N_a\delta_{ab}\Delta v_{bj}^n d\Omega,\end{aligned} \tag{35}$$

whereas the weak form of Eq. (30) expresses the velocity increment Δv_j of the solid phase as

$$\begin{aligned}\int_\Omega (1-n)\rho^s N_a\delta_{ab}\Delta v_{bj}d\Omega = &-\int_\Omega n\rho^l N_a\delta_{ab}\Delta w_{bj}d\Omega - \Delta t\int_\Omega \frac{\partial N_a}{\partial x_i}\sigma_{ij}^{'n}d\Omega \\ &- \Delta t\int_\Omega \frac{\partial N_a}{\partial x_j}p_a^n d\Omega + \Delta t\int_\Gamma N_a\left(\tau_{aj}^{'n} + N_a p_a^n n_j\right)d\Gamma + \Delta t\int_\Omega \rho g_j N_a d\Omega.\end{aligned} \tag{36}$$

The velocity of the solid phase at the next time step follows from the velocity at the current step and the velocity increment as $v_j^{n+1} = v_j^n + \Delta v_j$, and the same relation holds for the velocity of the liquid phase as $w_j^{n+1} = w_j^n + \Delta w_j$. In the integration points the pressure increase Δp, according to Eq. (31) is based on the liquid phase velocity at the next time step, and reads

$$n\beta\Delta p = n\Delta t\frac{\partial N_a}{\partial x_i}w_{ai}^{n+1} + (1-n)\Delta t\frac{\partial N_a}{\partial x_i}v_{ai}^{n+1}. \tag{37}$$

Finally the effective stress increase $\Delta\sigma'$ follows from Eq. (32) according to

$$\Delta\sigma'_{ij} = \tfrac{1}{2}\Delta t D_{ijkl}\left(\frac{\partial N_a}{\partial x_l}v_{ak}^{n+1} + \frac{\partial N_a}{\partial x_k}v_{al}^{n+1}\right). \tag{38}$$

Nodal velocity of the solid phase and nodal velocity of the liquid phase both follow from a forward time integration. The pressure and effective stress in the integration points follow from a backward relation with both velocities.

5 NUMERICAL SIMULATIONS

Limitations associated with various formulations have been discussed in detail in Chapter 1 of Pande & Zienkiewicz (1982). Two important factors are the period of response compared to the wave speed through a medium and the rate of drainage relative to the rate of loading. The examples given in his section are geared to specific aspects, namely the capability of capturing the second compression wave, and the impact on the solution associated with various assumptions. This section considers two cases, comparing solutions of the $v-p$ and the $v-w$ formulation for the simulation of the behavior of a confined soil column subjected to a surface load that is applied instantaneously. Since the emphasis is on wave propagation and dissipation of pore pressures the material is assumed to be linear elastic.

5.1 Case 1

For the first case a column is considered, in which the following mechanical properties apply: compression modulus of the water phase $K^l = 2000\,\text{MPa}$; bulk modulus of the skeleton $K = 2790\,\text{MPa}$ and shear modulus of the skeleton $G = 1650\,\text{MPa}$. The density of the solid phase $\rho^s = 2650\,\text{kg/m}^3$ and the density of the liquid phase $\rho^l = 1000\,\text{kg/m}^3$, with a porosity of the soil $n = 0.4$. As a result, we have an elasticity modulus of the mixture $E = K + \frac{4}{3}G + \frac{1}{n}K^l$ of $9990\,\text{MPa}$, with the speed of the compression wave given by

$$c_p = \sqrt{E/\rho}, \tag{39}$$

which for this case is $2241\,\text{m/s}$. The compression wave distributes the load over the liquid phase and the solid phase according to

$$p_0 = \frac{\alpha}{\alpha + n\beta}, \qquad \sigma_0' = \frac{n\beta}{\alpha + n\beta}, \tag{40}$$

where the compressibility of the liquid phase reads $\beta = 1/K^l$, and the compressibility of the solid phase follows from $\alpha = 1/\left(K + \frac{4}{3}G\right)$. For the parameters selected $p_0 = 0.5\sigma_0$ and $\sigma_0' = 0.5\sigma_0$.

The dynamic viscosity of the water phase μ is $1.0 \cdot 10^{-3}\,\text{Ns/m}^2$, the intrinsic permeability κ equals $1.0 \cdot 10^{-11}\,\text{m}^2$, and the gravitational acceleration g is set to $10\,\text{m/s}^2$. The hydraulic conductivity follows from the intrinsic permeability as $k = \kappa\rho^l g/\mu$. For the case at hand, as $k = 1.0 \cdot 10^{-5}\,\text{m/s}$, which applies for medium coarse sand. Given these parameters, the consolidation coefficient c_v follows from

$$c_v = \frac{k}{\rho^l g\,(\alpha + n\beta)}, \tag{41}$$

and equals $2.5\,\text{m}^2/\text{s}$.

The Courant criterion limits the time step Δt_1 for both the $v-p$ formulation and the $v-w$ formulation. As for the $v-p$ formulation a second criterion Δt_2 needs to be satisfied. Verruijt (2010) presented the time step criteria as

$$\Delta t_1 \leq \frac{1}{c_p}\Delta x, \qquad \Delta t_2 \leq \frac{1}{2c_v}\left(\Delta x\right)^2, \tag{42}$$

where Δx is the smallest element in the mesh. For a spatial discretization $\Delta x = 2.5\,\text{mm}$ the time steps should be restricted to $\Delta t_1 = 1.12 \cdot 10^{-6}\,\text{s}$ and $\Delta t_2 = 1.25 \cdot 10^{-6}\,\text{s}$.

Figure 1 compares $v-p$ simulation results to $v-w$ simulation results for the pore pressure and effective stress, in which the water pressure at the left side is set to $-1.0\,\text{Pa}$. In other words,

the increase in compressive stress at the left surface is entirely due to a water pressure change. The right side is fully fixed and impermeable. Both formulations capture the dynamic and the consolidation processes. The first process loads the liquid phase to a level of $-0.5\,\mathrm{Pa}$ and the second process gradually increases the liquid phase compressive pressure to $-1.0\,\mathrm{Pa}$, which corresponds to the total increase of the load at the boundary by raising the water level. The effective stress dissipates to its initial value of $0.0\,\mathrm{Pa}$ by consolidation. Verruijt (2010) presented the analytical solution for this problem and both $v-p$ simulation results and $v-w$ simulation results compare well to this solution.

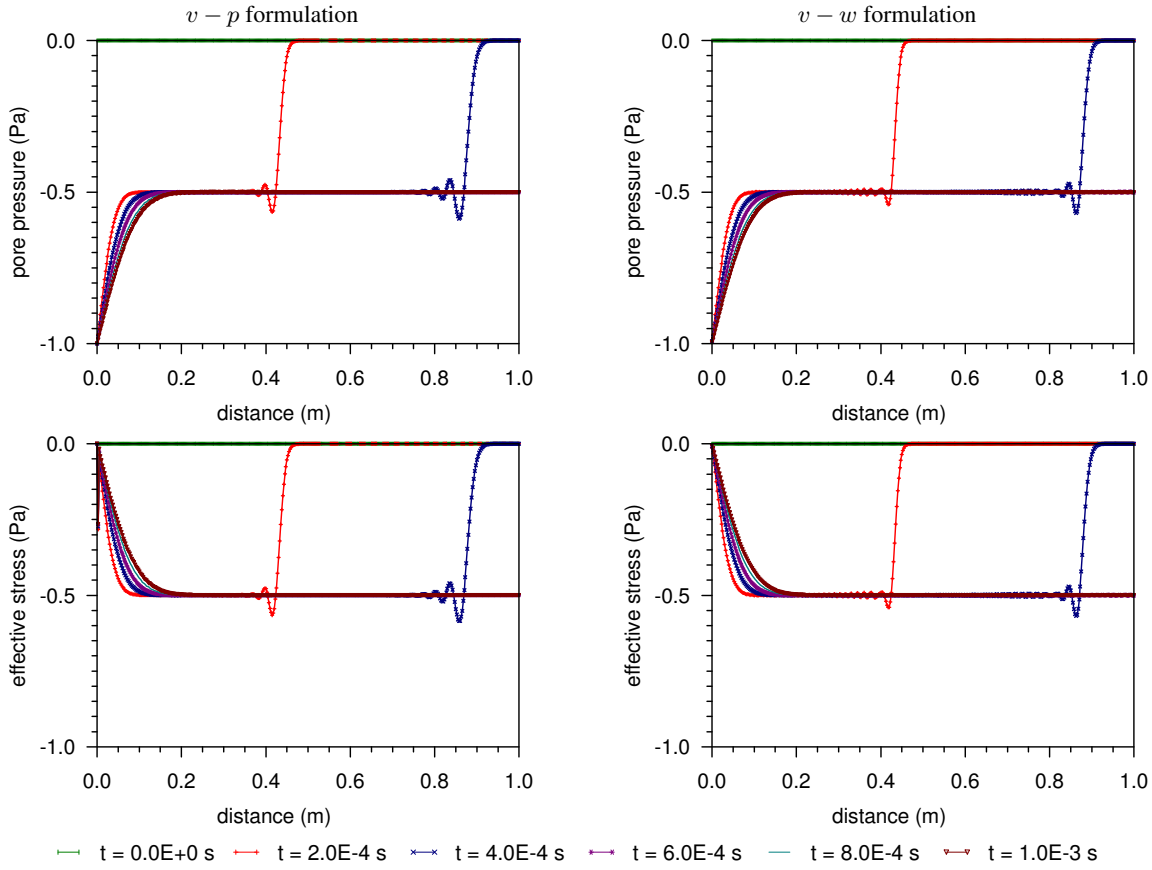

Fig. 1. Case 1, $v-p$ versus $v-w$ formulation results.

5.2 Case 2

For the second case the hydraulic conductivity is increased by a factor of 100, with the other parameters remaining the same. Owing to the increase in the hydraulic permeability, the consolidation coefficient equals $250\,\mathrm{m}^2/\mathrm{s}$. For a spatial discretization $\Delta x = 2.5\,\mathrm{mm}$ the second time step criterion becomes more restrictive: $\Delta t_2 = 1.25 \cdot 10^{-8}\,\mathrm{s}$.

Figure 2 compares $v-p$ simulation results to $v-w$ simulation results for the liquid phase and solid phase. The comparison clearly reveals a shortcoming with the $v-p$ formulation. The $v-w$ formulation is capable of capturing the first compression wave followed by a second wave that corresponds to the start of the consolidation process. The speed of the second wave is less than the speed of the first wave, and the second wave dissipates in space. Like the previous case, the first wave loads the liquid phase to a level of $-0.5\,\mathrm{Pa}$. The second wave increases the pressure

even further and decreases the effective stress as the total stress remains $-1.0\,\mathrm{Pa}$. The consolidation process increases the compressive water pressure to $-1.0\,\mathrm{Pa}$. This corresponds to the total increase of the load at the boundary by raising the water level. The effective stress dissipates to its initial value of $0.0\,\mathrm{Pa}$ by consolidation. Verruijt (2010) also presented the analytical solution for this problem. For this case $v-w$ simulation results compare well to the analytical solution. The $v-p$ formulation is not able to capture the second compression wave.

In order to take a closer look at what assumptions contribute to the difference, two additional simulations were performed with the $v-w$ formulation: (a) with $\partial w/\partial t \approx \partial v/\partial t$ in the momentum equation of the mixture and $\partial w/\partial t = 0$ in the momentum equation of the liquid; and (b) with $\partial w/\partial t \approx \partial v/\partial t$ in the momentum equation of the mixture only. For (a), it was found that the predictions were virtually identical to that of the $v-p$ formulation, whereas those for (b) were found to be similar to these of the full $v-w$ formulation. The peak total stress, was however found to be slightly larger. In other words, the difference between the formulations is attached to neglecting the acceleration of the fluid in the momentum balance equation of the fluid and not due to the use of a mixture acceleration.

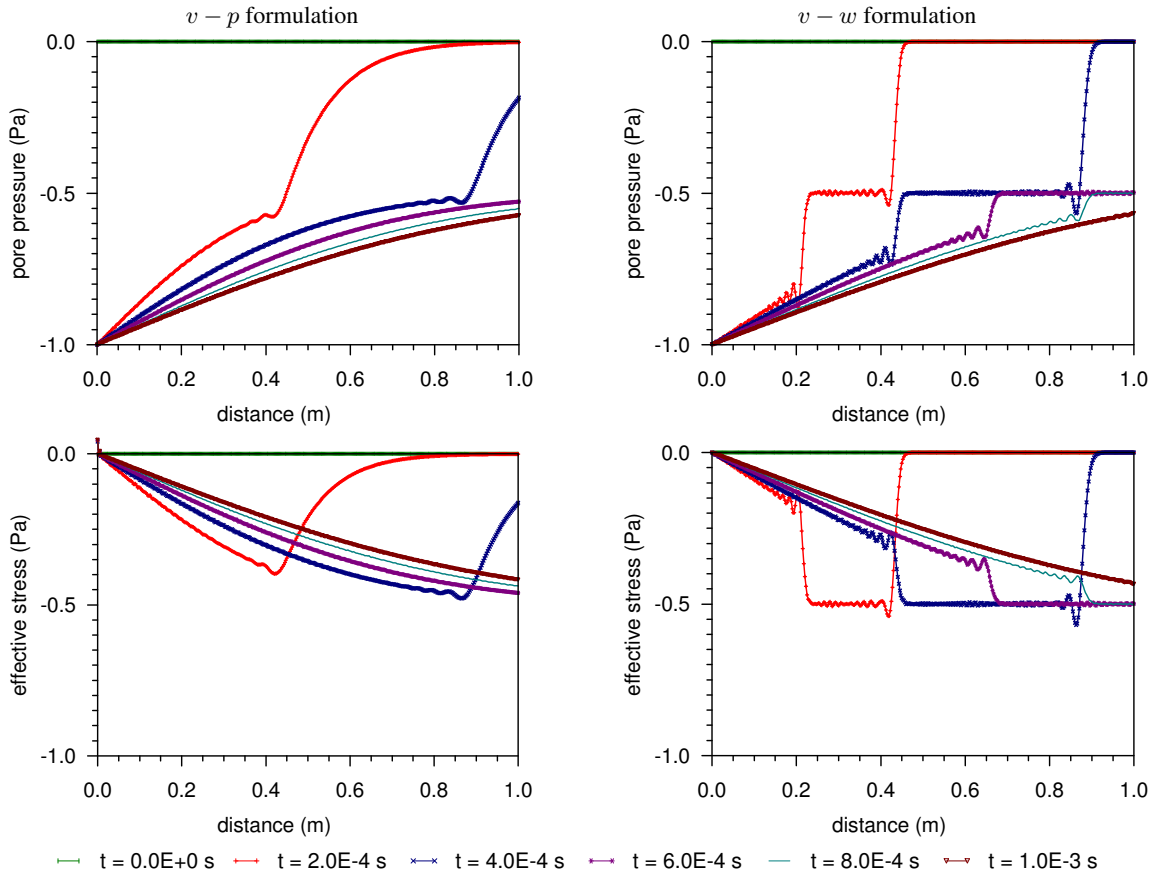

Fig. 2. Case 2, $v-p$ versus $v-w$ formulation results.

6 CONCLUSIONS

This article focused on explicit finite element models using low order elements, and being capable of properly capturing the physics of the dynamic response of a two-phase medium to dynamic loading. An important observation is that the fluid and solid velocities or displacements

are required as the degrees of freedom. For both $v-p$ and $v-w$ formulations a time stepping criterion that relates the critical time step to the spatial discretization size holds. However, for the $v-p$ formulation a second time stepping criterion has to be satisfied. This criterion relates to the square of the spatial discretization size and becomes more restrictive as the mesh size decreases. Because pressure relates to effective stress at the integration points, the $v-w$ formulations provides a more consistent form as both quantities follow as derivatives of nodal quantities. Only the $v-w$ formulation captures the second compression wave accurately.

The algorithms are being incorporated into a material point method framework. Use of fluid velocity as a primitive nodal unknown rather than pressure, which can be calculated at a material point, has the advantage that the algorithm for mapping information between the computation grid nodes and material points for the fluid is virtually identical to that for the solid phase. For example, the mapping of momentum from the material point to the nodes is tied to the physics (extensive thermodynamic property), unlike trying to map pressure (intensive thermodynamic property). There are however challenges when using low-order elements, namely mitigating locking that is associated with (near) incompressibility, and eliminating checker-boarding of the pressure field. Partial solutions to ongoing research are given by Stolle et al. (2009).

ACKNOWLEDGEMENT

This research was carried out as a part of the GEO-INSTALL project (Modelling Installation Effects in Geotechnical Engineering). It has received funding from the European Community through the program (Marie Curie Industry-Academia Partnerships and Pathways) under grant agreement no PIAP-GA-2009-230638.

REFERENCES

Biot, M. A. (1956a). Theory of propagation of elastic waves in a fluid-saturated porous solid. i. low-frequency range. *Journal of the Acoustical Society of America 28*(2), 168–178.

Biot, M. A. (1956b). Theory of propagation of elastic waves in a fluid-saturated porous solid. ii. higher frequency range. *Journal of the Acoustical Society of America 28*(2), 179–191.

Gidaspow, D. (1994). *Multiphase Flow and Fluidization Continuum and Kinetic Theory Descriptions*. Academic Press.

Jeremic, B., Cheng, Z., Taiebat, M., & Dafalias, Y. (2008). Numerical simulation of fully saturated porous materials. *International Journal for Numerical and Analytical Methods in Geomechanics 32*, 1635–1660.

Pande, G. & Zienkiewicz, O. (1982). *Soil Mechanics Transient and Cyclic Loads, Constitutive relations and numerical treatment*. John Wiley and Sons.

Stolle, D., Jassim, I., & Vermeer, P. (2009). Accurate simulation of incompressible problems in geomechanics. In M. Kuczma & K. Wilmanski (Eds.), *Lectures of the CMM 2009*, pp. 347–361. Springer Verlag.

Verruijt, A. (2010). *An Introduction to Soil Dynamics*, Volume 24 of *Theory and Applications of Transport in Porous Media*. Springer.

Zienkiewicz, O., Chan, A., Pastor, M., Paul, D., & Shiomi, T. (1990). Static and dynamic behaviour of soils: A rational approach to quantitative solutions, part i: Fully saturated problems. *Proceedings of the Royal Society 429*, 285–309.

Zienkiewicz, O. & Shiomi, T. (1984). Dynamic behavior of saturated porous media: the generalised biot formulation and its numerical solution. *International Journal for Numerical and Analytical Methods in Geomechanics 8*, 71–96.